

## Linear and nonlinear ac response in the superconducting mixed state

C. J. van der Beek

*Materials Science Division, Argonne National Laboratory, Argonne, Illinois 60439*

V. B. Geshkenbein

*Landau Institute of Theoretical Physics, Moscow, Russia*

V. M. Vinokur

*Materials Science Division, Argonne National Laboratory, Argonne, Illinois 60439*

(Received 8 March 1993)

The response of the vortex system in the mixed state of type-II superconductors to ac fields is discussed from a unique macroscopic point of view. Linear and nonlinear response are derived as two opposite limits of the same diffusionlike equation for magnetic flux. ac susceptibility experiments carried out in the limit of strong nonlinearity are entirely equivalent to magnetic-relaxation or field-ramp experiments. The magnitude and frequency dependence of the nonlinearity threshold, or amplitude of the ac field where one crosses from essentially linear to strongly nonlinear response, are found and discussed for both the vortex-liquid and vortex-glass states.

### I. INTRODUCTION

One of the most popular means of investigating vortex dynamics in the high-temperature superconductors (HTS's) is the measurement of the response of the vortex lattice (VL) to ac fields.<sup>1-7</sup> Such measurements have long been recognized as an important tool in the verification of models for pinning and motion of vortices in the mixed state of type-II superconductors.<sup>8-11</sup> ac techniques are generally more sensitive than dc-resistivity measurements as a result of the application of phase-sensitive detection and yield extra information since frequency can be varied in addition to temperature, dc field  $H_0$ , and ac-field amplitude.

The application of a time-dependent field  $\mathbf{H}(t) = \mathbf{H}_0 + \mathbf{h}_{ac} \exp(-i\omega t)$  to the sample surface results in an electric-field gradient in the sample interior ( $h_{ac}$  is the ac-field amplitude and  $\omega$  the angular frequency). This gives rise to a shielding current, which in turn exerts a Lorentz force on the vortices in the sample. The resulting vortex-displacement field  $\mathbf{u}(\mathbf{r}, t)$  modifies the distribution of magnetic induction  $\mathbf{B}$  and current density  $\mathbf{j}$  in the sample. Changes in the vector potential ( $\delta \mathbf{A}$ ) and in the induction ( $\delta \mathbf{B}$ ) that are due to vortex motion are connected to the displacement field by the relation<sup>12</sup>

$$\delta \mathbf{A} = \mathbf{u} \times \mathbf{B}, \quad (1)$$

$$\delta \mathbf{B} = \nabla \times \delta \mathbf{A}, \quad (2)$$

or

$$\delta \mathbf{B} = -\mathbf{B} \nabla \cdot \mathbf{u} + (\mathbf{B} \cdot \nabla) \mathbf{u} - (\mathbf{u} \cdot \nabla) \mathbf{B}. \quad (3)$$

The first two terms in Eq. (3) correspond to vortex-lattice compression and tilt, respectively.<sup>13</sup> The third term is of order  $\mathbf{u} \delta \mathbf{B}$  and may be dropped if we suppose that the change in field is much smaller than the field itself,

$\delta B \lesssim h_{ac} \ll B$ . The connection between  $\delta B$  and the vortex-displacement field means that measurement of the flux change  $\delta \Phi(t)$  near the sample, for instance, with a pickup coil or Hall probe,<sup>14</sup> can provide information on vortex dynamics.

Usually, the experiment is arranged in such a way that the induced voltage in the pickup coil or Hall probe is proportional to the (time-dependent) sample magnetic moment,

$$\mathcal{M}(t) = \int_{\text{sample}} \frac{1}{2c} \mathbf{r} \times \mathbf{j}(\mathbf{r}, t) d^3r. \quad (4)$$

It is then useful to express the ac response in terms of the ac susceptibility  $\chi$ , which is defined using the Fourier transform of  $\mathcal{M}(t)$ :

$$\chi = \sum_n \chi'_n + i\chi''_n, \quad (5)$$

$$\chi_n = \frac{1}{2\pi V h_{ac}} \int_0^{2\pi} \mathcal{M}(t) \exp(in\omega t) d\omega t \quad (6)$$

( $V$  is the sample volume). The imaginary component  $\chi''_1$  of the fundamental susceptibility has a special meaning in that it is a measure of the dissipation in the sample. Experiments on single-crystalline high-temperature superconductors show that upon ramping the temperature or dc magnetic field,  $\chi'_1$  varies monotonically from  $-1/4\pi$  to 0, while  $\chi''_1$  initially rises from zero, goes through a maximum, and then returns to a small value near  $T_c$ . The step in  $\chi'_1$  is due to the transition from near-perfect screening to complete penetration of the impinging ac field into the sample; the peak in  $\chi''_1$  marks the coincidence of the flux (current) penetration depth with the relevant sample dimension times a geometrical factor.<sup>15-17</sup> Also, the susceptibility curve has been found to depend on the ac-field frequency and in certain cases on the amplitude  $h_{ac}$ .

If the induced current  $\mathbf{j}(\mathbf{r}, t)$  is proportional to  $h_{ac} \exp(-i\omega t)$ , one speaks of linear response:  $\chi = \chi_1$ , and is independent of  $h_{ac}$ . Any other dependence of  $\mathbf{j}$  on  $h_{ac}$  leads to an amplitude-dependent susceptibility and necessarily to nonzero higher harmonics  $\chi_n$ . In a type-II superconductor, it is the presence of vortex pinning by crystal impurities which results in the appearance of a nonlinear ac magnetic response above a certain threshold driving-field amplitude<sup>11</sup> (note that the reverse, the absence of an observed driving-field dependence, does not necessarily imply the absence of significant pinning). The crossover between linear and nonlinear response has been observed in thin films and single crystals of  $\text{YBa}_2\text{Cu}_3\text{O}_{7-\delta}$  (YBCO) (Refs. 5, 18, and 19) and single crystals of  $\text{Bi}_2\text{Sr}_2\text{CaCu}_2\text{O}_8$  (BSCCO).<sup>6,20</sup> The onset of a higher harmonic response was reported for both YBCO and BSCCO crystals in Refs. 14 and 21. Both the linear-response regime and the regime of high amplitudes are relatively well understood, the first as arising from either an Ohmic resistive state in the sample<sup>13,16,17</sup> or from London-type electrodynamics, the latter in terms of the Bean critical-state model.<sup>9,22,23</sup> However, these two limits have often been considered as being based on completely different and unconnected and sometimes even conflicting approaches.<sup>19</sup>

The aim of this paper is to give a description of the linear as well as the nonlinear ac phenomena from a unique macroscopic point of view. We will see how both linear and nonlinear ac behavior arises as two different limiting cases of the same set of equations and find the position of the crossover between these two regimes.

## II. GENERAL DESCRIPTION OF ac VORTEX RESPONSE

We start with the Maxwell equations

$$\nabla \times \mathbf{E} = -\frac{1}{c} \frac{\partial \mathbf{B}}{\partial t}, \quad (7)$$

$$\nabla \times \mathbf{B} = \frac{4\pi}{c} \mathbf{j}. \quad (8)$$

In writing Eq. (8), it is supposed that the fields and current are quasistatic: All effects due to the finite velocity of propagation of electromagnetic disturbances are neglected. The Maxwell equations should be combined with the equation relating the current  $\mathbf{j}$  to the electric field  $\mathbf{E}$ , the latter being determined by the dynamic behavior of the superconductor. We write this relation in a form that is analogous to the case where  $\mathbf{E}$  is simply linear in  $\mathbf{j}$ ,

$$\mathbf{E} = \rho(\mathbf{j}, \omega, B, T) \mathbf{j}. \quad (9)$$

The resistivity  $\rho$  can be a complex and possibly nonlinear function of the current density  $\mathbf{j}$ . From Eqs. (7)–(9), one can easily derive the (nonlinear) diffusionlike equation for flux motion,

$$\frac{\partial \mathbf{B}}{\partial t} = \frac{c^2}{4\pi} [\nabla \rho(\mathbf{j}, \omega, B, T) \nabla] \mathbf{B}. \quad (10)$$

In order to describe the ac-susceptibility experiment, Eq. (10) should be solved for the case where the field

$\mathbf{H}(t) = \mathbf{H}_0 + \mathbf{h}_{ac} \exp(-i\omega t)$  (with  $h_{ac} \ll H_0$ ) is applied to the sample surface. The condition  $h_{ac} \ll H_0$  means that the change in  $\rho$  due to the change in  $B$  is negligible.

If  $\rho$  is independent of  $\mathbf{j}$ , Eq. (10) becomes the usual diffusion (heat-flow) equation.<sup>16,17</sup> We can then look for a solution of the type  $\mathbf{B} = \mathbf{H}_0 + \delta \mathbf{B}(\mathbf{r}, \omega) \exp(-i\omega t)$ , where  $\delta \mathbf{B}$  satisfies

$$\delta \mathbf{B} = \frac{ic^2 \rho}{4\pi \omega} \nabla^2 \delta \mathbf{B}. \quad (11)$$

Equation (11) defines the ac-penetration depth

$$\lambda_{ac} = \left[ \frac{ic^2 \rho(\omega, T)}{4\pi \omega} \right]^{1/2}. \quad (12)$$

This is related to the skin depth  $\delta$  by  $\lambda_{ac} = \delta \sqrt{i}$ .<sup>24</sup> In the case where  $\rho$  is independent of  $\omega$ , as in a normal metal, the penetration depth decreases with frequency as  $\lambda_{ac} \propto \omega^{-1/2}$ . As the frequency of the external ripple field is increased, the ac current and ac fields in the superconductor are then confined to a more narrow layer at the surface.

We can obtain Eq. (11) in another form by using Eqs. (2) and (8):

$$\delta \mathbf{A} = -\frac{4\pi \lambda_{ac}^2}{c} \mathbf{j}. \quad (13)$$

Thus  $\lambda_{ac}^{-2}$  is the response function relating the current density to the vector potential. If  $\lambda_{ac}^2$  is complex, there will be a phase lag of  $\mathbf{j}$  with respect to  $\delta \mathbf{A}$  at any point in the sample. This means that the response is hysteretic, leading to dissipation. From Eq. (13), one straightforwardly retrieves the electric field  $\mathbf{E} = -c^{-1} \delta \mathbf{A} = -4\pi ic^{-2} \omega \lambda_{ac}^2 \mathbf{j}$  and the frequency-dependent resistivity  $\rho = -4\pi ic^{-2} \omega \lambda_{ac}^2$ .

If the penetration depth is much smaller than the sample size, one can obtain the spatial field distribution inside the sample by approximating the surface as being flat.<sup>24</sup> The problem then reduces to finding the field distribution inside a conducting half space (e.g., occupying  $x > 0$ ). The solution is  $B(x, t) = H_0 + \delta B(x, t)$ , where  $\delta B(x, t) = h_{ac} \exp(-i\omega t - x/\lambda_{ac})$ . The real and imaginary parts of  $\lambda_{ac}$  can now be interpreted as describing the envelope of the penetrating induction and as a position-dependent phase factor between the external and internal fields, respectively. The current density is linear in the ac-field amplitude,

$$\begin{aligned} j(x, t) &= (ch_{ac}/4\pi \lambda_{ac}) \exp(-i\omega t - x/\lambda_{ac}) \\ &= c \delta B(x, t) / 4\pi \lambda_{ac}, \end{aligned}$$

the current density at the surface equals  $j_s = (ch_{ac}/4\pi \lambda_{ac}) \exp(-i\omega t)$ .

We now turn to the more general case where  $\rho$  is allowed to depend on  $\mathbf{j}$  and the response is nonlinear. A solution of Eq. (10) can now only be found for certain forms of  $\rho(\mathbf{j})$ .<sup>25</sup> We can, however, formally repeat the linear-response result and write down a general form for the ac-penetration depth,

$$\lambda_{ac} \simeq \frac{c}{4\pi} \frac{\delta B(x,t)}{j(x,t)} \simeq \left[ \frac{ic^2 \rho(j, \omega, B, T)}{4\pi\omega} \right]^{1/2}. \quad (14)$$

This form evidently becomes an exact equation in the linear limit. We shall argue that in the case of strong nonlinearity, Eq. (14) also provides a very accurate description of the current distribution.

Suppose, for instance, that the resistivity can be described by the thermally activated form

$$\rho(\omega=0, j) = \rho_0 \exp \left[ -\frac{U(j)}{k_B T} \right], \quad (15)$$

with  $U(j)$  the effective activation energy. The solution of Eq. (10) using this form of  $\rho$  was previously investigated analytically<sup>26,25</sup> and numerically<sup>27,28</sup> for an infinite slab (superconductor bounded by planes  $|x|=d/2$ ) in a constant field  $H_0$  applied parallel to the slab surface. The solution then corresponds to a shielding current that decays with time. In Ref. 27 the flux profile at  $t=0$  was chosen to represent the Bean critical state, in which  $j$  equals the critical-current density  $j_c$  over a surface shell of thickness  $H_0/j_c$ , whereas in Ref. 28 the initial flux profile was established by calculating the sample response to a field ramp at a constant rate  $\dot{H}$ , until  $H=H_0$  was reached. The changing magnitude of the magnetic field at the surface results in an electric-field gradient, which in turn induces a shielding current of magnitude  $j < j_c$  in the sample interior. The spatial variation of  $j$  is determined by the actual form of  $U(j)$ . If  $U(j)$  is a strongly nonlinear function of  $j$  (and does not depend explicitly on  $B$ ), the current density remains constant within a shell of thickness  $x_B = cH(t)/4\pi j$ . The flux profile in the region of penetration can thus be approximated by a straight line. The magnitude of  $j$  depends on the magnitude of the local electric field and therefore on the field sweep rate  $\dot{H}$ . It is given implicitly by the relation

$$U(j(\dot{H})) = k_B T \ln \left[ \frac{c^2 \rho_0 j}{4\pi x_B \dot{H}} \right]. \quad (16)$$

The straight-line approximation remains valid even after flux has penetrated to the center of the sample: The central region where the flux profile is not linear is exponentially small. The current density is again given by Eq. (16), but with  $d$  instead of  $x_B$  under the logarithm. If  $\rho(j)$  is a weakly varying function of  $j$ , the straight-line approximation is not valid: Results are then better approximated by linear-response theory. The parameter that measures the degree of nonlinearity is

$$r = \left| \frac{\partial U(j)}{\partial j} \right| \frac{j}{k_B T}. \quad (17)$$

If the change in  $\rho(j)$  due to a change in  $j$  is much greater than the relative change in  $j$  itself,  $r \gg 1$ , and one has strong nonlinearity. Conversely,  $r \ll 1$  means that  $\rho(j)$  [or  $U(j)$ ] can be treated as constant on the experimental time scale and the problem reduces to that of linear response.

We now return to the ac-susceptibility experiment,

which just corresponds to periodically ramping the field up and down between the values  $H_0 \pm h_{ac}$  at the rate  $\dot{H} = \omega h_{ac}$ . The current density should therefore behave in exactly the same way as in the field-ramp experiment. In the case of strong nonlinearity ( $r \gg 1$ ), the current density at  $\omega t = 0[\text{mod}(\pi)]$  is constant over a surface shell of thickness  $x_B = ch_{ac}/4\pi j(\omega)$ . The thickness  $x_B$  is actually the Bean ac-penetration length,<sup>9</sup> but with  $j_c$  replaced by  $j(\omega)$ . Substitution of the nonlinear resistivity (15) in the general formula for the penetration depth (14) yields the implicit relation, for the magnitude of  $j(\omega)$ ,

$$U(j(\omega)) = k_B T \ln \left[ \frac{1}{\omega\tau} \right], \quad (18)$$

where the relaxation time  $\tau = 4\pi(\delta B)^2/c^2\rho_0 j(\omega)^2$ . Equation (18) is the same as Eq. (16), with the replacement  $\dot{H} \rightarrow \omega\delta B$ .

The response in the case of strong nonlinearity ( $r \gg 1$ ) is thus characterized by an ac-penetration depth  $\lambda_{ac} = x_B$  that depends linearly on  $h_{ac}$  and a spatially constant current density  $j(\omega)$ . This should be contrasted to the linear limit where  $\lambda_{ac}$  is constant and  $j$  is proportional to  $h_{ac}$ . However, the two situations are linked as two different limits of the same solution of Eq. (10). The crossover from linear to nonlinear response will occur when  $r \approx 1$ . Because the ac current is strongest at the sample surface, nonlinear response will start there. It therefore suffices to consider the surface current density  $j_s = ch_{ac}/4\pi\lambda_{ac}$  when evaluating  $r$ .

### III. APPLICATION TO VARIOUS VORTEX STATES

We now consider the specific features characterizing the linear and nonlinear ac response in different parts of the mixed-state phase diagram. In each subsection we shall first review existing results for the linear response (small  $h_{ac}$ ) in order to establish the different frequency regimes. In the linear-response regime,  $\lambda_{ac}$  is determined by the behavior of the frequency-dependent resistivity  $\rho(\omega, j=0)$ . Next, these results will be extended to the nonlinear response (large  $h_{ac}$ ), where the response is dominated by the dc resistivity  $\rho(\omega=0, j)$ . It will be seen that the onset of nonlinearity in the ac response can be described in a manner completely analogous to the crossover between different frequency regimes of linear response, namely, by the equation of the relevant ac-penetration depths at the crossover.

#### A. Vortex liquid

The vortex-liquid state is characterized by a finite linear dc resistivity due to vortex motion,  $\rho(\omega=0, j=0) \neq 0$ . This implies that for  $j \rightarrow 0$ , the effective energy barriers for thermally activated vortex motion do not depend on the current density. The low-current activation barriers in the vortex liquid state are those associated with the plasticity of the vortex system,<sup>29</sup> possibly due to vortex entanglement:<sup>30</sup>  $U(j=0) = U_{pl}$ .

### 1. Linear response

If one subjects the sample to a low-amplitude ac field of very high frequency, but smaller than the gap frequency  $\Delta/\hbar$ , the ac-penetration depth is very small. Because the shielding current is confined to a thin surface layer, we can neglect the interaction with the vortices. The ac response can essentially be found from the London equation

$$\mathbf{j} = -\frac{c}{4\pi\lambda_L^2} \mathbf{A}, \quad (19)$$

which is just Eq. (13) with  $\lambda_{ac}$  equal to the London penetration depth  $\lambda_L$ . Because  $\lambda_L$  is real, there is no dissipation and  $\chi'_1 = 0$ .

As the frequency is lowered,  $\lambda_{ac}$  increases to the point where the interaction of the surface current with the vortices becomes important. The total vector potential

$$\mathbf{A} = -\frac{4\pi\lambda_L^2}{c} \mathbf{j} + \mathbf{u} \times \mathbf{B} \quad (20)$$

now consists of a part related to the surface-shielding current and a part due to vortex displacements. The vortex-displacement field  $\mathbf{u}(\mathbf{r}, t)$  can in principle be found from the solution of the appropriate equation of motion, e.g.,

$$-\eta\dot{\mathbf{u}} + F(\mathbf{u}, \mathbf{r}) + \frac{1}{c} \mathbf{j} \times \mathbf{B} = F_T(t). \quad (21)$$

Here  $\eta$  is the vortex-lattice flow viscosity and  $F_T(t)$  is a random thermal (Langevin) force. The restoring force  $F(\mathbf{u}, \mathbf{r})$  is the sum of the elastic force due to the other vortices and of the elementary forces  $f$  exerted by randomly distributed individual pinning centers. The equilibrium positions of the vortices correspond to local minima of potential energy, at which  $F(\mathbf{u}, \mathbf{r}) = 0$ . Evidently, these positions differ from the vortex-lattice sites occupied in the absence of pinning. The fact that pinning centers are randomly distributed means that the positions of local energy-minima are also random. Moreover, because pinning is a *collective* phenomenon (the restoring force also depends on vortex elasticity), the heights of the energy barriers *between* potential minima are also random. This means that, in practice, one is dealing with a *distribution* of restoring forces.

For small vortex excursions from local minima, the potential is harmonic, so that the restoring force is elastic. One writes  $F(\mathbf{u}, \mathbf{r}) = -\alpha_L(\mathbf{r})\mathbf{u}$ , where the "spring constant"  $\alpha_L(\mathbf{r})$  has been called the Labusch constant.<sup>31</sup> In this limit, Eq. (21) is linear and can in principle be solved. Assuming that  $\mathbf{u}(\mathbf{r}, t)$  can be written as  $\mathbf{u}(\mathbf{r})\exp(-i\omega t)$ , the formal solution neglecting thermal fluctuations is

$$\mathbf{u}(\mathbf{r}, t) = -\frac{1}{c} \frac{\mathbf{j}(\mathbf{r}) \times \mathbf{B}}{i\omega\eta - \alpha_L(\mathbf{r})} \exp(-i\omega t). \quad (22)$$

In order to calculate quantities such as the ac-penetration depth, one should take the average over disorder of  $\mathbf{u}$ , i.e., the average over the ensemble of  $\alpha_L$  values. Unfortunately, such a calculation is hindered by the fact that the distribution function for  $\alpha_L$  (i.e., for the restoring

force) is unknown. We will therefore suppose that the distribution of pinning potential barriers (between local minima) is characterized by a single typical energy value  $U$ . By also taking a single typical pinning interaction range  $r_f$ , one can estimate  $\alpha_L \approx U/Vr_f^2$ , where  $V$  is the volume of an independently pinned region of the VL.

For example, in the case of weak collective pinning due to randomly positioned point defects one expects a reasonably broad barrier distribution, where both the mean and width have the same energy scale  $U_c = [W(0)V_c]^{1/2}r_f$ . The pinning strength  $W(0) = n_p \langle f^2 \rangle$  is the product of the point-defect density  $n_p$  and the variance of the elementary pinning force over a unit cell of the VL.<sup>32</sup> The correlation volume  $V_c = R_c^2 L_c$  is the size of the region in which vortex displacements due to pinning are less than  $r_f$ . The lengths  $R_c$  and  $L_c$  are determined from the condition that the pinning energy  $[W(0)V_c]^{1/2}r_f$  equals the energy of elastic deformation over a distance  $u = r_f$ . The elastic energy equals  $c_{66}(r_f/R_c)^2$  and  $c_{44}(r_f/L_c)^2$  for shear and tilt deformations, respectively, where  $c_{66}$  and  $c_{44}$  are the vortex-lattice shear and tilt moduli. Because pinning is mainly due to the interaction of the vortex core with the defects, the pinning range is of the order of the core size: At fields  $B < 0.2B_{c2}$ ,  $r_f$  approximately equals the Ginzburg-Landau coherence length  $\xi$ , whereas at fields near  $B_{c2}$  it is given by the vortex spacing  $a_0$  (Ref. 33) ( $B_{c2}$  is the upper critical field). The typical value for the Labusch parameter can now be estimated as  $\langle \alpha_L \rangle \approx U_c/V_c r_f^2$ . It is more convenient to express  $\langle \alpha_L \rangle$  in terms of the critical-current density,  $j_c = [W(0)/V_c]^{1/2}/B$ , which is an experimentally accessible quantity. We then have  $\langle \alpha_L \rangle = j_c B / r_f$ .

Whereas the concepts of weak collective pinning are thought to be applicable in the low-temperature vortex-glass state, in the vortex-liquid phase the barriers were conjectured to be those for plastic motion of portions of the VL. There is a narrow distribution of barrier heights with a typical value  $U_{pl}$ . For sufficiently short times, the concept of a critical-current density still makes sense, so that we can again write  $\langle \alpha_L \rangle = j_c B / r_f$ .

The solution of Eq. (21) leads to three frequency regimes of vortex-dominated response (see Fig. 1). From Eq. (22) one sees immediately that for  $\omega \gg \omega_0 \equiv \langle \alpha_L \rangle / \eta$ , one has  $\omega\eta \gg \alpha_L$ ; i.e., the effect of viscous drag dominates over the restoring force. The quantity  $\omega_0$  is called the "pinning frequency." Neglecting the restoring force altogether, we use Eq. (1) to write the vector potential  $\delta \mathbf{A} = -(iB^2/c\eta\omega)\mathbf{j}$ . Comparing this to Eq. (13), we have the ac-penetration depth

$$\lambda_{ac} \approx \lambda_{FF} = \left[ \frac{iB^2}{4\pi\eta\omega} \right]^{1/2} \propto \omega^{-1/2}(1+i). \quad (23)$$

$\lambda_{ac}$  is complex, as in a normal metal with resistivity  $\rho_{FF} \equiv B^2/\eta$ . Both  $\chi'_1$  and  $\chi''_1$  are nonzero.<sup>34</sup>

At frequencies below  $\omega_0$ , the restoring force  $-\alpha_L \mathbf{u}$  dominates over the viscous-drag force, which can then be neglected. If thermal fluctuations are also not important, we have  $\alpha_L \mathbf{u} = \mathbf{j} \times \mathbf{B} / c$  and the displacement can be ob-

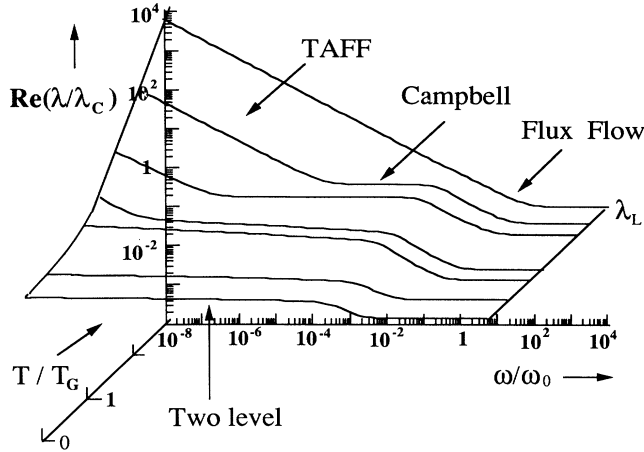


FIG. 1. Real part of the ac-penetration depth, plotted as function of frequency and temperature, showing the qualitative behavior in the various vortex states.

tained immediately. In order to obtain the ac-penetration depth, one must take the average of  $\mathbf{u}$  over disorder,  $\langle \mathbf{u} \rangle = (\mathbf{j} \times \mathbf{B}/c) \langle \alpha_L^{-1} \rangle$ . Taking the cross product with  $\mathbf{B}$  on either side yields Eq. (13) with  $\lambda_{ac}$  equal to the Campbell penetration depth,<sup>11</sup>

$$\lambda_{ac} \approx \lambda_C \equiv \left[ \frac{B^2}{4\pi} \langle \alpha_L^{-1} \rangle \right]^{1/2}. \quad (24)$$

Because  $\lambda_C$  is real and frequency independent, the ac response is essentially London-like: The sample behaves as a true superconductor, but with a larger penetration depth or a “reduced superfluid density.” The ac-field penetration is carried by reversible vortex oscillations near their equilibrium positions. The resistivity  $\rho(\omega) \approx -4\pi ic^{-2} \omega \lambda_C^2$ . Note that, at the frequency  $\omega_0$  where the crossover from flux-flow (FF) to Campbell response takes place,  $\lambda_C = \lambda_{FF}$ .

At frequencies below  $\omega_0 \exp(-U_{pl}/k_B T)$ , thermally activated vortex jumps between most favorable metastable states of the vortex lattice come into play. One should now take both the random thermal force  $F_T(t)$  and the behavior of the restoring force  $F(\mathbf{u}, \mathbf{r})$  for arbitrary displacement into account in Eq. (21). After solving for  $\mathbf{u}(\mathbf{r}, t)$ , the result should again be averaged over disorder, whence one faces the same problem as before. For a qualitative description of the low-frequency behavior, we use the assumption that the barrier distribution is narrow and can be characterized by a single energy scale  $U_{pl}$ . Thermally activated flux motion is accounted for by a linear average vortex velocity

$$\dot{u}_{TAFF} = (c\rho_0 j / B) \exp(-U_{pl}/k_B T).$$

This means that this response will be similar to that in the high-frequency flux-flow regime. Because of the activated nature of flux motion, one speaks of “thermally assisted flux flow (TAFF).”<sup>16</sup> The low-frequency resistivity can be written as

$$\rho(\omega) \approx \rho_{TAFF} \equiv \rho_0 \exp\left[-\frac{U_{pl}}{k_B T}\right], \quad (25)$$

which remains finite as  $\omega \rightarrow 0$ ,  $j \rightarrow 0$ . It is the presence of this contribution to the linear resistivity that characterizes the vortex-liquid state. The complex ac-penetration depth becomes

$$\lambda_{ac} \approx \lambda_{TAFF} \equiv \left[ \frac{ic^2 \rho_{TAFF}}{4\pi\omega} \right]^{1/2}; \quad (26)$$

the ac response is the same as the skin effect in a normal metal with resistivity  $\rho_{TAFF}$ . The crossover to Campbell-type response takes place when  $\lambda_{TAFF} = \lambda_C$ .

A “general” form for the ac-penetration depth has been obtained by adding  $\dot{u}_{TAFF}$  to the velocity containing flux-flow and Campbell contributions only [the time derivative of Eq. (22)].<sup>7,35</sup> One then obtains

$$u = -\frac{jB}{c} \left[ \frac{\alpha_L}{1-i/\omega\tau_1} + i\omega\eta \right]^{-1}. \quad (27)$$

The relaxation time  $\tau_1 \equiv B^2/\alpha_L \rho_{TAFF}$  is defined by  $\lambda_{TAFF}(\omega = \tau_1^{-1}) = \lambda_C$ . A more thorough approach was employed by Coffey and Clem.<sup>36</sup> These authors solved the vortex equation of motion (21) self-consistently, where they took  $F(u, r)$  as the gradient of a *periodic* potential with fixed barrier height  $U$ . Their analysis yields a very complete description of the linear-vortex response in the above-mentioned four frequency regimes. Their final result for the vortex displacement is just Eq. (27), but with  $\tau_1 = (\eta/\alpha_L) I_0^2(U/2k_B T)$ , where  $I_0(x)$  is the modified Bessel function. This closely resembles an exponential for large argument  $x$ .

While the results<sup>36</sup> describe experimental data in the vortex-liquid regime quite well, it should be noted that by taking a periodic potential with fixed barrier height the authors<sup>36</sup> also implicitly depart from the assumption that the problem may be described using a typical restoring-force constant rather than a random one. It remains unclear whether such a description yields the same results as the full treatment based on solving Eq. (21) with a random restoring force and performing the correct thermal and disorder averages.

## 2. Nonlinear response

We now move to the case where an ac-field amplitude is applied that is sufficiently high to bring the system into the regime of strongly nonlinear response. At sufficiently low frequencies ( $\omega\tau_1 < 1$ ), the dc resistivity is of the form (15) with a typical barrier height  $U_{pl}$ . The resistivity becomes strongly nonlinear near the characteristic current  $j_c$ . Applying Eq. (17), one has

$$r \approx \frac{j}{j_c} \frac{U_{pl}}{k_B T}. \quad (28)$$

Crossover from linear (TAFF) to nonlinear [“flux-creep” (FC)] response takes place when  $r \approx 1$ . The change in the vortex free energy due to the induced current then becomes of the order of the thermal energy. The surface

current density below the onset of nonlinearity is  $j_s \approx ch_{ac}/4\pi\lambda_{\text{TAFF}}$ , so that the nonlinearity threshold in terms of the ac-field amplitude becomes

$$h_{ac} > h_{\text{FC}} = \frac{4\pi}{c} j_c \lambda_{\text{TAFF}} \left[ \frac{k_B T}{U_{\text{pl}}} \right] \propto \omega^{-1/2}. \quad (29)$$

Inserting values typical for the vortex liquid,  $j_c = 1 \times 10^4 \text{ A cm}^{-2}$ ,  $U_{\text{pl}}/k_B T = 10$ , and  $\rho_0 = 1 \mu\Omega \text{ cm}$  yields a value  $h_{\text{FC}} \sim 10^2 (\omega/[s^{-1}])^{-1/2} \text{ Oe}$ . Note that at the nonlinearity threshold  $\lambda_{\text{TAFF}}$  equals the ‘‘Bean penetration length’’  $x_B = ch_{ac}/4\pi j_T$ , with  $j_T \equiv j_c (k_B T/U_{\text{pl}})$  determined by the temperature. The threshold amplitude  $h_{\text{FC}}$  decreases with increasing frequency [see Fig. 2(a)]. This is because the surface shell (of width  $\lambda_{ac}$ ) in which the shielding currents are confined becomes narrower for larger  $\omega$ , so that the surface current density increases. Furthermore, the value of  $h_{\text{FC}}$  increases roughly exponentially with temperature. At temperatures  $T > U_{\text{pl}}/k_B$  pinning becomes irrelevant and the equality  $r = 1$  cannot be satisfied at current densities  $j < j_c$ . One is then always in the linear-response regime. This is also true for experiments carried out at frequencies  $\omega < c^2 \rho_{\text{TAFF}}/(4\pi d^2)$  [or,

equivalently,  $\omega\tau_1 < (\lambda_c/d)^2$ ], where  $d$  is a characteristic sample dimension.<sup>16</sup> In fact, at these temperatures and frequencies,  $j_c$  does not exist at all.<sup>29</sup>

At frequencies  $\omega\tau_1 > 1$ , the probability of thermally activated jumps at low ac amplitudes (in the linear regime) is negligible, the ac response is determined by vortex oscillations near equilibrium (Campbell regime), and  $\lambda_{ac} = \lambda_c$ . The ac resistivity is linear and purely imaginary; the dc resistivity is zero. At high amplitudes, the vortex lattice is depinned. The resistivity is strongly nonlinear and real. We therefore cannot use an activated form of the resistivity [such as Eq. (15)] to describe the response for arbitrary  $h_{ac}$ . By consequence, the amplitude at which the crossover from linear to strongly nonlinear response takes place should be estimated in a slightly different way.

Let us briefly consider the nonlinearity threshold in the ‘‘vortex solid’’ at  $T = 0$ , where a similar situation arises. Below the critical-current density  $j_c$ , one has Campbell-type response, while above  $j_c$  the resistivity is Ohmic. Rather than using Eq. (15) (which has no meaning at  $T = 0$ ), we model the dc resistivity by using the form  $\rho(\omega = 0, j) = \rho_0 \Theta(j - j_c)$ , where  $\Theta(x)$  is the Heaviside step function. The general ac-penetration depth is written

$$\lambda_{ac} \approx \frac{c\delta B}{4\pi j} \approx \left[ \frac{c^2 \rho_0 \Theta(j - j_c)}{4\pi \omega} \right]^{1/2}; \quad (30)$$

the equivalent of Eq. (18) is

$$\Theta(j - j_c) = \frac{4\pi \omega (\delta B)^2}{c^2 \rho_0 j^2} \equiv \omega \tau. \quad (31)$$

As in Eq. (18), nonlinear response arises when the relative change in  $\rho(\omega = 0, j)$  due to a change in  $j$  is greater than the relative change in  $j$  itself. Clearly, this can only be so when  $j \approx j_c$ . Because below crossover the surface current density  $j_s = ch_{ac}/4\pi\lambda_c$ , nonlinearity is observed when<sup>11</sup>

$$h_{ac} \gtrsim \frac{4\pi}{c} j_c \lambda_c = (4\pi j_c B r_f)^{1/2} \approx (H_0 H_{c1})^{1/2} \left[ \frac{j_c}{j_0} \right]^{1/2} \equiv h_p. \quad (32)$$

Here  $j_0 = \Phi_0/2\sqrt{3}\pi\lambda^2\xi$  is the depairing current,  $H_{c1}$  is the lower critical field,  $r_f$  was taken to equal  $\xi$ , and we have used the relation  $\lambda_c^2 = B^2 r_f/4\pi j_c$ . The parameter values  $j_c \approx 1 \times 10^6 \text{ A cm}^{-2}$ ,  $j_0 \approx 10^8 \text{ A cm}^{-2}$ , and  $H_{c1} \approx 150 \text{ Oe}$  yield  $h_p \approx 10^2 (B/[T])^{1/2} \text{ Oe}$ .

At  $h_{ac} = h_p$ , the Campbell length  $\lambda_c$  equals the Bean length  $x_B = ch_{ac}/4\pi j_c$ . The ac-field amplitude at which crossover from a Campbell-type response to the Bean critical state takes place can thus be estimated by comparing the penetration lengths in each regime. Also, one can see from Eq. (3) that at  $h_p$  the amplitude of vortex oscillations at the sample surface is roughly equal to the characteristic length scale of the pinning potential,  $u_s \approx r_f$ . This is the length at which the anharmonicity of the pinning potential becomes important.

Returning to the vortex liquid and nonzero temperatures, one can distinguish two situations. Namely, for in-

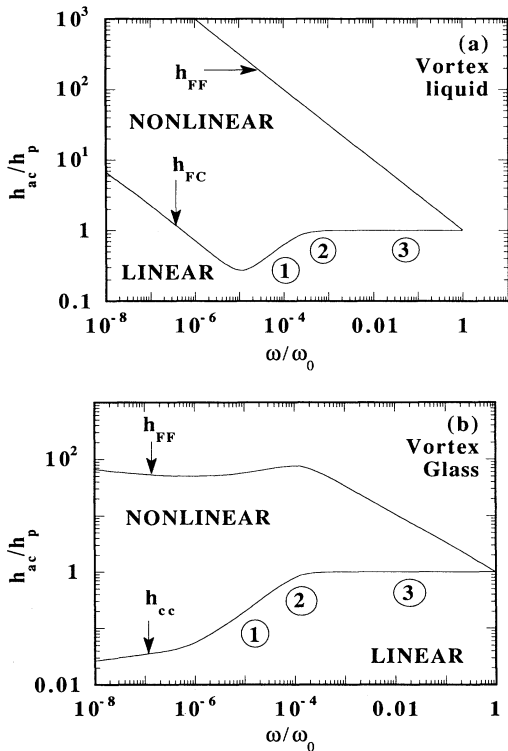


FIG. 2. Regimes of linear and nonlinear vortex ac response in (a) the vortex liquid ( $U_{\text{pl}}/k_B T = 10$ ) and (b) the vortex glass ( $U_c/k_B T = 10$ ). The solid lines correspond to different crossover criteria mentioned in the text. In (a) the labels 1, 2, and 3 refer to the conditions  $\omega\tau_1 \gtrsim 1$  (intervalley jumps at high amplitudes only),  $\omega\tau_{\text{ph}} \lesssim 1$  (no activated jumps, but  $j_c$  suppressed by thermal fluctuations), and  $\omega\tau_{\text{ph}} \approx 1$ , respectively. In (b) the labels refer to the corresponding conditions with  $\tau_1$  replaced by  $\omega_0^{-1} \exp(U_c/k_B T)$ .

intermediate frequencies  $\omega\tau_1 \gtrsim 1$  [region 1 in Fig. 2(a)], there is an appreciable probability for thermally activated jumps, but only for high ac amplitudes. The result for the vortex solid can now immediately be generalized. At current densities  $j \lesssim j_c$ , the activation barrier can be expanded in  $j$ :  $U(j) = U_{\text{pl}}(1 - j/j_c)$ . The current in the limit of strong nonlinearity can be derived using Eq. (18),

$$j(\omega) \approx j_c \left[ 1 - \frac{k_B T}{U_{\text{pl}}} \ln \left[ \frac{1}{\omega\tau} \right] \right]. \quad (33)$$

Equating  $j_s = j(\omega) = h_{\text{ac}}/\lambda_C$  yields the nonlinearity threshold

$$h_{\text{ac}} \gtrsim \frac{4\pi}{c} j(\omega) \lambda_C = h_p \left[ 1 - \frac{U_{\text{pl}}}{k_B T} \ln \left[ \frac{1}{\omega\tau} \right] \right] \quad (\omega\tau_1 \gtrsim 1). \quad (34)$$

This criterion corresponds to  $\lambda_C = x_B(\omega) = ch_{\text{ac}}/4\pi j(\omega)$  or, alternatively, to  $|\rho(\omega, j=0)| = \rho(\omega=0, j)$ . The vortices become depinned at a smaller value of the displacement,  $u_s \approx r_f [1 - (k_B T/U_{\text{pl}}) \ln(1/\omega\tau)]^2$ .

When the frequency is increased to values  $\omega \lesssim \omega_0$  [region 2 in Fig. 2(b)], activated jumps between minima of the random potential can be neglected for all values of  $h_{\text{ac}}$  and in the strongly nonlinear limit  $j$  simply equals  $j_c$ . However,  $j_c$  can be considerably suppressed with respect to its “zero-temperature” value because of phononlike thermal fluctuations in the vortex positions.<sup>37</sup> Thermal fluctuations smear out the pinning potential, rendering it less effective. In Ref. 37 it was shown that the effect of thermal fluctuations can be taken into account by replacing the pinning range  $r_f \approx \xi$  by an effective range  $\xi_T = (\xi^2 + \langle u^2 \rangle_T)^{1/2}$  in the expression for  $j_c(B, T)$ . Here  $\langle u^2 \rangle_T$  is the mean-square thermal vortex displacement in the absence of pinning. The resulting strongly-temperature-dependent form of  $j_c(B, T)$  should be substituted in Eq. (32). Further estimates should include the frequency spectrum of thermal fluctuations: At higher experimental frequencies, the mean thermal vortex displacement per ac-field cycle is smaller, smearing of the random potential is less, and the measured  $j_c$  is larger. The frequency spectrum in the absence of pinning follows a Lorentzian  $\langle u^2(\omega) \rangle_T \propto (1 + \omega\tau_{\text{ph}})^{-1}$ , with

$$\tau_{\text{ph}} \approx \left[ \frac{\lambda_L}{\lambda_{\text{FF}}} \right]^2 \omega^{-1} \approx \frac{\lambda_L^2 \eta}{c_{11}(0)}, \quad (35)$$

the relaxation time for compressional waves (a typical vortex-lattice phonon frequency).<sup>29,38</sup> In HTS's,  $\tau_{\text{ph}} \sim 10^{-10}$  s.

The implications for the nonlinearity threshold are that it should start to deviate downward from the form (34) when  $\omega$  increases above  $\tau_{\text{ph}}^{-1} \exp(-U_{\text{pl}}/k_B T)$ . Its frequency dependence becomes less as frequency increases, until it reaches the value  $h_p$  when  $\omega\tau_{\text{ph}} \sim 1$  [region 3 in Fig. 2(a)].

It is interesting to consider the effect of increasing  $h_{\text{ac}}$  ever further once one is in the nonlinear limit. At current densities  $j \gtrsim j_c$ , pinning is irrelevant,  $U(j) \equiv 0$ , and the condition  $r < 1$  is also satisfied. The resistivity

$\rho(\omega, j \gtrsim j_c) = \rho_{\text{FF}}$ , so that the ac response is the same as in the high-frequency flux-flow regime. At crossover,  $j_s \approx ch_{\text{ac}}/4\pi\lambda_{\text{FF}} \approx j_c$  or

$$h_{\text{ac}} \approx \frac{4\pi}{c} j_c \lambda_{\text{FF}} = \left[ \frac{4\pi j_c B^2}{\eta\omega} \right]^{1/2} = h_p \left[ \frac{\omega_0}{\omega} \right]^{1/2} \equiv h_{\text{FF}}. \quad (36)$$

The above parameter values, together with  $\eta \approx 1 \times 10^5 / (B/[T])^2$  P/cm<sup>3</sup>, yield  $h_{\text{FF}} \approx 10^3 (B\omega^{-1}/[T\text{s}])^{1/2}$  T, meaning that the sketched situation may be relevant in a pulsed high-field experiment. Note that when  $\omega \approx \omega_0$ ,  $h_{\text{FF}} \approx h_p$ , and the nonlinear regime collapses. Thus (as long as  $j < j_0$ ) the response is always linear in both the flux-flow and London-response frequency regimes, which is a direct consequence of the irrelevance of vortex pinning at these frequencies

### B. ac response near the vortex-glass transition

It has been suggested<sup>39,40</sup> that [in three-dimensional (3D) systems] there exists a finite-temperature phase transition (at temperature  $T_G$ ) separating the vortex liquid from a vortex-glass (VG) state. We briefly review the ac response near this phase-transition line, before describing the behavior in the vortex-glass phase in detail.

From the critical scaling hypothesis, it was found that near the VG phase transition, the nonlinear resistivity should scale as  $\rho(\omega=0, j) \propto j^{(z-D+2)/D-1}$ , where  $z$  is the dynamic critical exponent and  $D$  is spatial dimensionality.<sup>40</sup> Experiments<sup>41,42</sup> have shown that  $z \approx 5$ . The nonlinear resistivity can be written as

$$\rho(\omega=0, j) = \rho_0 \exp \left[ \frac{z-D+2}{D-1} \ln(j) \right],$$

and hence the parameter  $r = (z-D+2)/(D-1) \approx 2$ .

If one is near to, but above  $T_G$ , the low-frequency linear resistivity is still determined by the plastic behavior of the vortex liquid (TAFF):  $\rho(\omega, j=0)$  is complex and frequency independent. Above a certain current density

$$j_{\text{pl} \rightarrow G} \sim (\rho_{\text{TAFF}}/\rho_0)^{D-1/(z-D+2)}$$

however,  $\rho_{\text{TAFF}} > \rho(\omega=0, j)$  and one crosses over to glassy response. The “effective activation barrier” is thus constant below  $j_{\text{pl} \rightarrow G}$  ( $U = U_{\text{pl}}$ ,  $r=0$ ) and drops as  $\ln(1/j)$  above it ( $r=2$ ). Hence the response becomes nonlinear near  $j_{\text{pl} \rightarrow G}$  or when

$$h_{\text{ac}} \gtrsim h_{\text{pl} \rightarrow G} \sim \frac{4\pi}{c} j_{\text{pl} \rightarrow G} \lambda_{\text{TAFF}} \sim \omega^{-1/2}. \quad (37)$$

This criterion, much similar to Eq. (29), again yields a nonlinearity threshold that decreases with increasing frequency and increases with temperature.

At higher frequencies the linear ac resistivity near the transition was argued to scale as<sup>40</sup>

$$\rho(\omega, j=0) \sim -i\omega^{(z-D+2)/z}. \quad (38)$$

The corresponding penetration depth

$$\lambda_G = \left[ \frac{ic^2 \rho(\omega, j=0)}{4\pi\omega} \right]^{1/2} \sim \omega^{(2-D)/2z}, \quad (39)$$

is real, and the ac response is London like. The behavior of  $\lambda_G = \lambda_{ac}(T = T_G)$  is illustrated in Fig. 1. The crossover to nonlinear response can be determined from  $|\rho(\omega, j=0)| = \rho(\omega=0, j)$ . The crossover current density follows  $j \equiv j_G \sim \omega^{(D-1)/z}$ . The ac susceptibility becomes amplitude dependent when

$$h_{ac} \gtrsim h_G = \frac{4\pi}{c} j_G \lambda_G \sim \omega^{D/2z}. \quad (40)$$

Assuming that  $z \approx 5$  for  $D=3$ ,  $\lambda_G \sim \omega^{-0.1}$ ,  $j_G \sim \omega^{0.4}$ ,<sup>42</sup> and  $h_G \sim \omega^{0.3}$ . This behavior is much similar to that in the Campbell regime in the vortex liquid.

### C. Vortex glass

In contrast to the vortex liquid, the vortex-glass state is characterized by a vanishing dc linear resistivity at zero current density,  $\rho(\omega=0, j=0)=0$ . This means that the flux-creep activation barriers diverge for  $j \rightarrow 0$ . We will take the vortex glass to be weakly pinned by the collective interaction with randomly distributed point defects. The distribution of barrier heights between metastable states is broad. It is centered around the typical energy  $U_c$  and the width is also of order  $U_c$ . In Ref. 43 it was shown that for such a system the relevant activation barriers at current density  $j$  are given by  $U(j) = U_c(j_c/j)^\alpha$ . In an ac experiment, the relevant barriers are those that can be overcome in a time  $t = \omega^{-1}$ , i.e., those that satisfy Eq. (18). Thus the relevant energy barriers become arbitrarily large as frequency decreases. The form of the distribution function means, however, that their density simultaneously decreases.

#### 1. Linear response

The linear ac response at frequency  $\omega > \omega_0$  is necessarily similar to that in the vortex liquid because pinning is irrelevant in either case. The Campbell regime will also be similar provided that the pinning potential is harmonic for small vortex displacements. We can, however, make use of the results of collective-pinning theory to relate the Campbell penetration depth to the dimensions of the correlation volume  $V_c$  transverse and parallel to  $\mathbf{B}$ ,  $R_c$ , and  $L_c$ . If pinning is sufficiently weak,  $R_c > \lambda_L$  and we can neglect the dispersion of the elastic constants (local limit). In the case of a sample of infinite thickness (3D collective pinning), the correlation lengths are related through<sup>32</sup>

$$L_c = R_c \left[ \frac{c_{44}(0)}{c_{66}} \right]^{1/2} = \frac{4\pi c_{44}(0) c_{66} r_f^2}{W(0)}. \quad (41)$$

Here  $c_{44}(0) = BH/4\pi \approx B^2/4\pi$  is the vortex-lattice tilt modulus in the local limit. Writing  $\langle \alpha_L \rangle = [W(0)/V_c]^{1/2}/r_f$  in Eq. (24) and eliminating  $R_c$ , we find

$$\lambda_{C,loc} \approx L_c. \quad (42)$$

When the condition  $R_c > \lambda_L$  does not hold, the nonlocal expressions for the elastic moduli and correlation lengths should be used. In this case,  $L_c$  and  $R_c$  grow exponentially with  $B$ . Experiments on  $\alpha\text{-Mo}_x\text{Si}$  and  $\alpha\text{-Nb}_x\text{Ge}$  films<sup>44</sup> have shown, however, that a 3D vortex lattice in the presence of disorder is unstable to the nucleation of screw dislocations. A better description is the ‘‘amorphous limit’’ in which flux lines are pinned independently and  $R_c$  equals the vortex-lattice parameter  $a_0 \approx (\Phi_0/B)^{1/2}$  ( $\Phi_0$  is the flux quantum). Using the estimates<sup>45</sup> for the (nonlocal) tilt modulus in the amorphous limit,  $c_{44A} \approx \Gamma^{-1} c_{44}(0) a_0^2 / \lambda_L^2$  ( $\Gamma \equiv m_z/m$  is the material anisotropy parameter), we find

$$\lambda_{C,A} \approx \Gamma^{1/2} \left[ \frac{\lambda_L}{a_0} \right] L_{C,A}. \quad (43)$$

Finally, in the case of a thin film of thickness  $d < L_c$ , we have 2D collective pinning, and

$$\lambda_{C,2D} \approx R_c \left[ \frac{c_{11}(0)}{c_{66}} \right]^{1/2}, \quad (44)$$

where  $c_{11}(0) = B^2/4\pi$  is the local VL compression modulus.

Since in the vortex-glass phase the TAFF regime is absent, the main qualitative difference between the vortex glass and the vortex liquid manifests itself at low frequencies,  $\omega < \omega_0 \exp(-U_c/k_B T)$ . Because we now have a broad distribution of barriers, the relevant ones [to be denoted by  $U(\omega)$ ] are given by Eq. (18). In the low-current (linear) limit, activation barriers are large. Vortices can perform one jump per ac cycle only, so that the main contribution to the ac response comes from pairs of metastable states. This means that the vortex configuration in the random field can be viewed as a set of two-level systems.

The two-level (TL) response of the vortex system was recently described by Koshelev and Vinokur<sup>46</sup> (see also Refs. 40 and 47). The  $i$ th pair of metastable states can be characterized by the volume  $V_i \sim L_i^d$  of the VL involved in the jump (‘‘fluxon bundle’’), the displacement  $u_i \sim r_f (L_i/L_c)^\xi$ , the energy barrier  $U_i$  separating the two states, and the energy difference  $\Delta_i$  between states.  $d$  is the dimensionality of the activated VL volume, and  $\xi$  is the wandering exponent. The bundle volume and the energy barrier are determined from the condition that  $U_i$  be of the order of the energy of elastic deformation,  $C(u_i/L_i)^2 L_i^d$ . One then finds that  $U_i = U_c (L_i/L_c)^{d-2+2\xi}$ . For a single-vortex line ( $d=1$ ),  $\xi=0.6$ ,  $C=c_{44A}$ , and  $L_i$  is the length of the displaced vortex-line segment, for a 2D bundle,  $\xi \approx 0.4$ ,  $C=c_{66}$ , and  $L_i$  is the transverse dimension of the vortex bundle, while for a 3D bundle  $\xi$  is estimated at 0.2, and  $C \approx c_{44}$  if we take  $L_i$  as the longitudinal size of the bundle.<sup>43</sup>

The barriers that contribute most to flux motion are those for which  $U_i \approx U(\omega)$ . The ac-penetration depth can now straightforwardly be estimated by equating the magnitude of the relevant activation barrier to the energy



gain due to the driving force,  $U(\omega) = jBL(\omega)^d u(\omega)/c$ . From Eqs. (1) and (13), we have  $j = (c/4\pi)uB/\lambda_{ac}^2$  and hence

$$\lambda_{ac}^2 = \frac{B^2}{4\pi} \frac{u^2 L^d}{U(\omega)}. \quad (45)$$

In the case of local elasticity, we can substitute the above relations between  $u$ ,  $L$ , and  $U$ . Making use of the fact that  $U_c = c_{44}(0)(r_f/L_c)^2 L^d$ , the penetration depth becomes

$$\lambda_{TL,loc} = L = L_c \left[ \frac{U(\omega)}{U_c} \right]^{-1/\psi} \quad (46)$$

$$= \lambda_c \left[ \frac{k_B T}{U_c} \ln \left[ \frac{1}{\omega\tau} \right] \right]^{-1/\psi}, \quad (47)$$

where  $-\psi = d - 2 + 2\xi$  and  $\tau$  is the same as in Eq. (18).

In the amorphous limit (single-vortex pinning), the situation is somewhat different. An expression for  $\lambda_{ac}$  in this limit was derived in Ref. 46. It is the same as Eq. (47), but with  $\psi = (2\xi - 1)/(2\xi - 3)$ .

The ac-penetration depth depends weakly on frequency (see Fig. 1). Because the real part of  $\lambda_{TL}$  is much larger than the imaginary part, the response is similar to that in the Campbell regime. When  $\lambda_{TL} = \lambda_c$ , or  $\omega\tau = \exp(-U_c/k_B T)$ , one expects a crossover to a oscillatory vortex response.

## 2. Nonlinear response

In the vortex-glass state, the resistivity in the strong nonlinear limit can be written in the form (15), where the effective activation barrier for flux creep  $U(j) = U_c(j_c/j)^\alpha$ . The exponent  $\alpha = (d + 2\xi - 2)/(2 - \xi)$ .<sup>43</sup> If we apply the crossover criterion (17), we find that response is linear for  $\alpha U(j) < k_B T$  or  $j > j_c(\alpha U_c/k_B T)^{1/\alpha}$ . Since in the vortex glass  $U_c \gg k_B T$ , Eq. (17) yields the more or less trivial result of the linear response at current densities  $j \gg j_c$ . The current density above crossover is  $ch_{ac}/4\pi\lambda_{FF}$ ; hence, in the vortex glass,

$$h_{FF} = \frac{4\pi}{c} j_c \lambda_{FF} \left[ \alpha \frac{U_c}{k_B T} \right]^{1/\alpha}. \quad (48)$$

In the limit of small current densities, the application of Eq. (17) yields a nonlinear dc response down to arbitrarily low  $j$ . In an ac experiment, however, one has the linear two-level response, so that the onset of nonlinearity is again qualitatively similar to that in the Campbell regime in the vortex liquid: One is in the nonlinear limit when  $j_s = j(\omega) = ch_{ac}/4\pi\lambda_{TL}$ . The current density  $j(\omega)$  in the strongly nonlinear limit is obtained from Eq. (18):

$$j(\omega) = j_c \left[ \left[ \frac{k_B T}{U_c} \ln \left[ \frac{1}{\omega\tau} \right] \right] \right]^{1/\alpha}. \quad (49)$$

Using the above result for  $\lambda_{TL}$ , we find that the crossover from two-level response to collective creep (CC) occurs when

$$h_{ac} \gtrsim h_{CC} \equiv \frac{4\pi}{c} j(\omega) \lambda_{TL} = h_p \left[ \frac{k_B T}{U_c} \ln \left[ \frac{1}{\omega\tau} \right] \right]^{-1/\alpha - 1/\psi}. \quad (50)$$

The behavior of  $h_{CC}$  as function of frequency and temperature depends on the value of  $d$  and  $\xi$ . Using the appropriate combinations for 2D ( $d=2$ ,  $\xi \approx 0.4$ ) or 3D ( $d=3$ ,  $\xi \approx 0.2$ ) bundles and the single-vortex line ( $d=1$ ,  $\xi=0.6$ ), it is seen that the sum  $\alpha^{-1} + \psi^{-1}$  is always positive, and hence  $h_{CC}$  increases with increasing frequency [see Fig. 2(b)]. Furthermore,  $h_{CC}$  should decrease with increasing  $T$ . This behavior is qualitatively opposite to that found in the vortex-liquid state. Because of the large value of  $U_c/k_B T$  in the vortex-glass state, the magnitude of  $h_{CC}$  can be much smaller than that of  $h_p$ . For example, in the single-vortex regime,  $\alpha^{-1} + \psi^{-1} = 2$ . A typical value for HTS's,  $U_c/k_B T \approx 10$ , then yields  $h_{CC} \approx 0.01 h_p$  [see Fig. 2(b)].

Finally, one can consider the crossover to nonlinearity from the Campbell regime. As in the vortex-liquid state, one has an intermediate-frequency regime  $\omega\tau \gtrsim \exp(-U_c/k_B T)$  and a high-frequency regime  $\omega \lesssim \omega_0$ . Applying the same consideration as in the vortex liquid, the nonlinear threshold at intermediate frequencies is

$$h_{ac} > \frac{4\pi}{c} j(\omega) \lambda_c = h_p \left[ \frac{k_B T}{U_c} \ln \left[ \frac{1}{\omega\tau} \right] \right]^{1/\alpha}. \quad (51)$$

At high frequencies one can use the collective pinning results<sup>46,37</sup> for the temperature dependence of  $j_c$  and  $\lambda_c(T)$  to estimate  $h_p = (4\pi/c)j_c\lambda_c$ .

The behavior of the nonlinearity threshold in the vortex-glass state is shown in Fig. 2(b).

## IV. DISCUSSION

Upon comparing the ac response of the vortex liquid to that of the vortex glass, it is seen that a qualitative difference only exists in the low-frequency regime where thermally activated intervalley jumps are important. Since the linear response of both the vortex liquid<sup>36</sup> and the vortex glass<sup>46</sup> have been extensively discussed in the past, we will focus on the limit of strongly nonlinear response. The threshold ac field where one enters the nonlinear limit was derived above. Note that while in the vortex liquid the nonlinearity threshold decreases with frequency and increases with temperature, in the vortex glass the behavior is opposite. Provided that the measurement frequency  $\omega\tau < \exp(-U/k_B T)$ , a measurement of the onset of nonlinearity at different frequencies can thus immediately distinguish between a vortex glass and a vortex liquid. In the vortex-glass phase, the condition  $r \gg 1$  can be easily satisfied at any temperature: The nonlinearity threshold is typically of the order of 1–10 Oe.

As pointed out in Sec. II, an ac experiment in the limit of strong nonlinearity ( $r \gg 1$ ) is equivalent to a magnetization hysteresis [ $M(H, \dot{H})$ ] measurement. The current density in the sample is almost constant over the region of penetration, a surface shell of thickness  $x_B = ch_{ac}/4\pi j(\omega)$ . The magnitude of the shielding current

can be obtained from Eq. (18). In an infinitely long sample with the field applied along the surface or for small flux penetration, this means that the flux profile is linear. Hence one can use the Bean model to describe the experiment, but with  $j_c$  replaced by  $j(\omega)$ . For example, the ac susceptibility in the case of an incompletely penetrating ac field parallel to the surface of an infinite slab of thickness  $d$  can be straightforwardly derived from the formulas given in Refs. 9 and 22. Taking the example of the vortex glass, one has

$$\chi'_1 = \frac{ch_{ac}}{4\pi j(\omega)d} = \frac{ch_{ac}}{4\pi j_c d} \left[ \frac{k_B T}{U_c} \ln \left[ \frac{1}{\omega\tau} \right] \right]^{1/\alpha}, \quad (52)$$

$$\chi''_1 = \frac{ch_{ac}}{3\pi^2 j(\omega)d} = \frac{ch_{ac}}{3\pi^2 j_c d} \left[ \frac{k_B T}{U_c} \ln \left[ \frac{1}{\omega\tau} \right] \right]^{1/\alpha}. \quad (53)$$

Now the relaxation time  $\tau \approx 4\pi h_{ac}^2 / c^2 \rho_{FF} j^2$ , which corresponds to the sample  $L/R$  time. Expressions for  $h_{ac} > (4\pi/c)j(\omega)d$  and for higher harmonics can be derived similarly using Refs. 9 and 22.

As long as the inequality  $r \gg 1$  holds, we can use modified versions of the Bean model<sup>22</sup> to describe the susceptibility for an arbitrary sample geometry. The susceptibility will be some function of the parameter  $x_B/d = ch_{ac}/4\pi j(\omega)d$ , where  $d$  is the sample dimension in the direction along which flux penetration takes place. This means that in experiment,  $h_{ac}$  and  $\omega$  are interchangeable variables. For example, in the case where  $j(\omega)$  is described by Eq. (49), one can retrieve the original susceptibility result after a frequency change  $\omega \rightarrow \omega'$  by changing the amplitude by a factor  $[\ln(\omega\tau)/\ln(\omega'\tau)]^{1/\alpha}$ . The interchangeability of  $\omega$  and  $h_{ac}$  is true in particular for the position of the peak in  $\chi''$ . The peak occurs just when the ac current has penetrated the sample to a distance  $d/2$ . The condition  $x_B/d = \frac{1}{2}$  permits the current density to be estimated accurately. If one finds the combinations of  $h_{ac}(\omega)$  that preserve the position of the  $\chi''$  peak, one obtains a curve  $j(\omega) = ch_{ac}(\omega)/2\pi d$  that is equivalent to the magnetization relaxation curve  $j(t)$ .

The prime advantage of using this ac method to measure the time dependence  $j(t)$  [or current dependence  $U(j(t))$ ] is the greatly enhanced dynamic time range. The possibility of varying the frequency from 1 to  $10^6$  Hz in principle yields a range of six decades in time, more than can be achieved in dc-relaxation experiments, which can be carried out over a time window of usually three decades in the range 1– $10^5$  s. The combination of ac and dc techniques yields a vast range of times over which the behavior of  $j(t)$  can be checked. Finally, because  $h_{ac} \ll B$ , the ac experiment is carried out with an almost constant induction in the sample. Only for this situation

do analytic expressions for the current density in the sample exist.<sup>25</sup> A disadvantage of the technique is that the process of finding matching  $h_{ac}(\omega)$  values is rather tedious.

In contrast to measurements of  $j(t)$  [or  $U(j)$ ], finding the critical-current density  $j_c(B, T)$  requires that thermally activated jumps be unimportant. ac experiments provide a way to “freeze out” flux creep by increasing frequency until one is well in the (linear) Campbell regime ( $\omega \lesssim \omega_0$ ). The true temperature dependence of  $j_c$  may then be determined from  $\lambda_c(T)$ . This means that, in principle, ac-response measurements can separate the behavior of  $U(B, T)$  from that of  $j_c(B, T)$ , which is inherently impossible in dc magnetization experiments.<sup>28</sup>

## V. SUMMARY

We have outlined the unique macroscopic approach to vortex ac response in type-II superconductors, which comprises both linear and strongly nonlinear limits. In the linear regime, the response is similar to the skin effect, whereas in the nonlinear limit, the current density is spatially almost constant over the region of penetration. In a sample with a small demagnetizing factor, this means that the flux profile can be approximated by a straight line. There exists a smooth crossover between the two limits. The ac-field amplitude  $h_{ac}$  at which crossover takes place can be found by comparing the expressions for the ac-penetration depth in either limit. The crossover exists only at frequencies below the pinning frequency  $\omega_0$ , that is, at those frequencies where pinning is relevant. Measurements of the onset of the nonlinear ac response provides a means of distinguishing between vortex-liquid and vortex-glass behavior. Furthermore, low-frequency ac experiments in the limit of strong nonlinearity are equivalent to magnetic-relaxation measurements, but can be used to find the behavior of  $j(t)$  and  $U(j)$  over a wider parameter range. At high frequencies one should in principle be able to determine  $j_c(B, T)$  from the Campbell penetration depth.

## ACKNOWLEDGMENTS

We wish to thank M. V. Feigel'man and A. E. Koshelev for discussions. This work was supported by the U.S. Department of Energy, BES-Materials Sciences, under Contract No. W-31-109-ENG-38. C. J. van der Beek and V. M. Vinokur acknowledge support from the NSC funded Science and Technology Center for Superconductivity (Cooperative Agreement No. DMR91-20000).

<sup>1</sup>A. P. Malozemoff, T. K. Worthington, Y. Yeshurun, F. Holtzberg, and P. H. Kes, Phys. Rev. B **38**, 7203 (1988).

<sup>2</sup>J. van den Berg, C. J. van der Beek, P. H. Kes, and J. A. Mydosh, M. J. V. Menken, and A. A. Menovsky, Supercond. Sci. Technol. **1**, 242 (1989).

<sup>3</sup>A. Gupta, P. Esquinazi, H. F. Braun, and H. W. Neumüller,

Europhys. Lett. **10**, 663 (1989).

<sup>4</sup>P. L. Gammel, J. Appl. Phys. **67**, 4676 (1990).

<sup>5</sup>J. H. P. M. Emmen, G. M. Stollman, and W. J. M. de Jonge, Physica C **169**, 418 (1990).

<sup>6</sup>J. H. P. M. Emmen, V. A. M. Brabers, and W. J. M. de Jonge, Physica C **176**, 137 (1991).

- <sup>7</sup>C. J. van der Beek and P. H. Kes, Phys. Rev. B **43**, 13032 (1991).
- <sup>8</sup>Ph. Seng, R. Gross, U. Baier, M. Rupp, D. Koelle, R. P. Huebener, P. Schmitt, G. Saemann-Ischenko, and L. Schultz, Physica C **192**, 403 (1992).
- <sup>9</sup>C. P. Bean, Rev. Mod. Phys. **2**, 31 (1964).
- <sup>10</sup>J. I. Gittleman and B. Rosenblum, Phys. Rev. Lett. **16**, 734 (1966).
- <sup>11</sup>A. M. Campbell, J. Phys. C **2**, 1492 (1969); **4**, 3186 (1971).
- <sup>12</sup>B. D. Josephson, Phys. Rev. **152**, 211 (1966).
- <sup>13</sup>E. H. Brandt, Z. Phys. B **80**, 167 (1990).
- <sup>14</sup>J. Gilchrist and M. Konczykowski (unpublished).
- <sup>15</sup>J. R. Clem, H. R. Kerchner, and T. S. Sekula, Phys. Rev. B **14**, 1893 (1976).
- <sup>16</sup>P. H. Kes, J. Aarts, J. van den Berg, C. J. van der Beek, and J. A. Mydosh, Supercond. Sci. Technol. **1**, 242 (1989).
- <sup>17</sup>V. B. Geshkenbein, V. M. Vinokur, and R. Fehrenbacher, Phys. Rev. B **43**, 3748 (1991).
- <sup>18</sup>L. Krusin-Elbaum, L. Civale, F. Holtzberg, A. P. Malozemoff, and C. Feild, Phys. Rev. Lett. **67**, 3156 (1991).
- <sup>19</sup>L. Civale, T. K. Worthington, L. Krusin-Elbaum, and F. Holtzberg, in *Magnetic Susceptibility of Superconductors and other Spin Systems*, edited by R. A. Hein *et al.* (Plenum, New York, 1991).
- <sup>20</sup>C. J. van der Beek, M. Essers, P. H. Kes, M. J. V. Menken, and A. A. Menovsky, Supercond. Sci. Technol. **5**, S260 (1992).
- <sup>21</sup>D. M. Xenikos and T. R. Lemberger, Phys. Rev. B **41**, 869 (1989).
- <sup>22</sup>L. Ji, R. H. Sohn, G. C. Spalding, C. J. Lobb, and M. Tinkham, Phys. Rev. B **40**, 10936 (1989).
- <sup>23</sup>M. W. Johnson, D. H. Douglass, and M. F. Bocko, Phys. Rev. B **44**, 7726 (1991).
- <sup>24</sup>L. D. Landau and E. M. Lifshitz, *Electrodynamics of Continuous Media, Course of Theoretical Physics*, Vol. 8 (Pergamon, New York, 1960), Sec. 45.
- <sup>25</sup>V. M. Vinokur, M. V. Feigel'man, and V. B. Geshkenbein, Phys. Rev. Lett. **67**, 915 (1991); V. B. Geshkenbein, M. V. Feigel'man, and V. M. Vinokur, Physica C **185-189**, 2511 (1991).
- <sup>26</sup>M. V. Feigel'man, V. B. Geshkenbein, and V. M. Vinokur, Phys. Rev. B **43**, 6263 (1991).
- <sup>27</sup>C. J. van der Beek, G. J. Nieuwenhuys, P. H. Kes, H. G. Schnack, and R. P. Griessen, Physica C **197**, 320 (1992).
- <sup>28</sup>H. G. Schnack, J. G. Lensink, R. P. Griessen, C. J. van der Beek, and P. H. Kes, Physica C **197**, 337 (1992).
- <sup>29</sup>V. M. Vinokur, M. V. Feigel'man, V. B. Geshkenbein, and A. I. Larkin, Phys. Rev. Lett. **65**, 259 (1990).
- <sup>30</sup>D. R. Nelson, Phys. Rev. Lett. **60**, 1973 (1988); D. R. Nelson and H. S. Seung, Phys. Rev. B **39**, 9153 (1989).
- <sup>31</sup>R. Labusch, Cryst. Latt. Defects **1**, 1 (1969).
- <sup>32</sup>A. I. Larkin and Yu. N. Ovchinnikov, J. Low Temp. Phys. **21**, 409 (1979).
- <sup>33</sup>E. H. Brandt, Phys. Rev. Lett. **57**, 1347 (1986).
- <sup>34</sup>We can use the result (23) to estimate the crossover frequency between London-type and vortex-dominated ac response. From Ref. 17, we have the BCS dirty-limit result  $\delta = \lambda_L [2\pi\Delta \tanh(\Delta/2T)\rho(\omega)/\hbar\omega\rho_n]^{1/2}$ , where  $\rho_n$  is the normal-state resistivity. Equating  $\delta\sqrt{i}$  to  $\lambda_{FF}$  and using  $\eta \approx BB_{c2}/\rho_n$ , one finds the crossover at  $\omega \sim 2\pi(\Delta/\hbar)(B/B_{c2})$ .
- <sup>35</sup>E. H. Brandt, Phys. Rev. Lett. **67**, 2219 (1991).
- <sup>36</sup>M. W. Coffey and J. R. Clem, Phys. Rev. Lett. **67**, 386 (1991); Phys. Rev. B **45**, 9872 (1992).
- <sup>37</sup>M. V. Feigel'man and V. M. Vinokur, Phys. Rev. B **41**, 8986 (1990).
- <sup>38</sup>E. H. Brandt, Physica C **162-164**, 115 (1989).
- <sup>39</sup>M. P. A. Fisher, Phys. Rev. Lett. **62**, 1415 (1989).
- <sup>40</sup>D. S. Fisher, M. P. A. Fisher, and D. A. Huse, Phys. Rev. Lett. **43**, 130 (1991).
- <sup>41</sup>R. H. Koch, V. Foglietti, W. J. Gallagher, G. Koren, A. Gupta, and M. P. A. Fisher, Phys. Rev. Lett. **63**, 1511 (1989).
- <sup>42</sup>H. K. Olsson, R. H. Koch, W. Eidelloth, and R. P. Robertazzi, Phys. Rev. Lett. **66**, 2661 (1991).
- <sup>43</sup>M. V. Feigel'man, V. B. Geshkenbein, A. I. Larkin, and V. M. Vinokur, Phys. Rev. Lett. **63**, 2303 (1989).
- <sup>44</sup>P. H. Kes and R. Wördenweber, Phys. Rev. B **34**, 494 (1986).
- <sup>45</sup>P. H. Kes and J. van der Berg, in *Studies of High Temperature Superconductors*, edited by A. V. Narlikar (Nova Science, New York, 1989).
- <sup>46</sup>A. E. Koshelev and V. M. Vinokur, Physica C **175**, 465 (1991).
- <sup>47</sup>K. H. Fischer and T. Natterman, Phys. Rev. B **43**, 10372 (1991).